Crystal Structure of μ_4-Oxo-hexakis(μ-acetato)tetrazinc and Thermal Studies of its Precursor, Zinc Acetate Dihydrate*

Lassi Hiltunen,[a] Markku Leskelä,[b] Milja Mäkelä[a] and Lauri Niinistö[a,§]

[a]Laboratory of Inorganic and Analytical Chemistry, Helsinki University of Technology, SF-02150 Espoo and [b]Department of Chemistry and Biochemistry, University of Turku, SF-20500 Turku, Finland

Hiltunen, L., Leskelä, M., Mäkelä, M. and Niinistö, L., 1987. Crystal Structure of μ_4-Oxo-hexakis(μ-acetato)tetrazinc and Thermal Studies of its Precursor, Zinc Acetate Dihydrate. – Acta Chem. Scand., Ser. A 41: 548–555.

The structure of the title compound was redetermined using X-ray diffractometer data collected at 293 K for a single crystal grown by condensing the oxoacetate vapor. The compound crystallizes in the cubic space group *Fd3m* with a = 16.402(1) Å, V = 4412.6(8) Å^3 and Z = 8. Anisotropic refinement gave R = 0.037 for 304 reflections corrected for absorption. The $Zn_4O(CH_3COO)_6$ molecule has a central oxygen atom which is tetrahedrally coordinated to four zinc atoms. Each zinc atom is tetrahedrally surrounded by four oxygen atoms: three from different bidentate acetato groups [Zn–O = 1.946(4) Å], with the fourth one being the central oxygen [1.936(1) Å]. Other structures with μ_4-oxygen in the center of a metal atom tetrahedron are also discussed.

The thermal behaviour of zinc acetate dihydrate was investigated by thermoanalytical methods (TG, DSC, DTA) and by mass spectrometric studies. Zinc acetate has a considerable vapor pressure above 180 °C which makes it a possible candidate for thin-film growth of zinc chalcogenides by the Atomic Layer Epitaxy (ALE) technique. High growth rates are obtained because the condensation of anhydrous zinc acetate leads to formation of the tetrameric phase $Zn_4O(CH_3COO)_6$ which then sublimes.

The oxoacetates of beryllium and zinc possess some physical properties which are uncommon for most simple metal complexes, viz. high volatility without decomposition, and solubility in organic solvents but not in water. The exceptional characteristics of the oxoacetates aroused interest already at the turn of the century[1] and later led to attempts to use the beryllium compound in purification of the metal and in chromatographic separations.[2,3] The covalent nature of the oxoacetate complexes has been attributed to the unusual coordination whereby the metal atoms are at the corners of an oxygen-centered tetrahedron and the acetato groups form bridges between the metal atoms at the edges. The early structural predictions[4–7] were confirmed later by Saito *et al.*,[8,9] who showed that in the isomorphous compounds the tetrahedral arrangement is rather regular, with Be–O and Zn–O distances ranging from 1.61 to 1.65 Å and from 1.96 to 1.98 Å, respectively.[8] The accuracy of the X-ray determinations was low (R = 0.18)[9] according to present day standards, however.

Our interest in zinc carboxylates stems from a search for new volatile starting materials to be used for growing electroluminescent zinc sulfide thin films by the Atomic Layer Epitaxy (ALE) method.[10,11] The conventional zinc source in the industrial process is zinc chloride, which has a relatively low volatility requiring growth temperatures around 500 °C. Replacing zinc chloride by zinc acetate resulted, indeed, in lower growth temperatures and simultaneously increased the growth rate.[12] The mechanism of volatilization and thin-film growth turned out to be much more complicated than in the case of zinc chloride,[13]

*Presented at the *XII Nordiska Strukturkemistmötet* in Sånga-Säby, Sweden, June 8–13, 1987.

§To whom correspondence should be addressed.

however, and prompted us to undertake the present detailed structural and thermoanalytical investigation.

Experimental

Materials. Zinc acetate dihydrate was an analytical reagent from E. Merck, Darmstadt, and it was used as such in thin-film growth experiments by the ALE process.[12] Single crystals of $Zn_4O(CH_3COO)_6$ up to 1 mm in length were obtained originally from the condensate in the ALE reaction chamber; an additional batch was prepared by vacuum evaporation and condensation of zinc acetate vapor. Zinc oxoacetate forms white octahedrally shaped crystals which melt at 252–3 °C. The crystals are somewhat sensitive to atmospheric moisture.

X-Ray measurements. X-ray intensity data were collected at room temperature on a Syntex $P2_1$ automatic four-circle diffractometer using Mo$K\alpha$ radiation. Details of crystal data and structure refinement are presented in Table 1. After the final cycles of refinement a difference electron density map was calculated, but attempts to locate the methyl hydrogen atoms at expected locations were unsuccessful. Tables of observed and calculated structure factors and anisotropic thermal parameters are available from the authors upon request.

Table 1. Summary of crystal data, intensity collection and structure refinement for $Zn_4O(CH_3COO)_6$.

Crystal data	
Formula	$Zn_4O(CH_3COO)_6$
Mol. wt.	631.8
Crystal system	Cubic
Space group	$Fd3m$ (No. 227)
a/Å	16.402(1)
V/Å^3	4412.6(8)
Z	8
d_{calc}/Mg m^{-3}	1.902
Radiation	Mo$K\alpha$ (λ = 0.71069 Å)
μ(Mo$K\alpha$)/cm^{-1}	44.35
Crystal size/mm	0.25×0.20×0.20
Data collection and structure refinement	
2θ scan speed/°min^{-1}	Variable 1–30 (θ/2θ)
No. of data collected	384 ($3 < 2\theta < 60$)
No. of unique data [$I_{obs} > 3\sigma(I_{obs})$]	304
Abs. correction (empirical, ψ-scan)	Min. trans. factor range 0.60–0.92 (max. trans. 1.0)
No. of variables	20
R	0.037
$R_w[w = 1/\sigma^2(F)]$	0.034

Thermoanalytical experiments. TG and DTG curves were recorded in a dynamic nitrogen atmosphere with Perkin-Elmer Series 2 and 7 thermogravimetric instruments, respectively, connected to the TADS data station. DSC curves were recorded with DSC-4 and DSC-7 instruments from the same manufacturer and were evaluated using the TADS programs. Simultaneous recording of the TG and DTA curves together with EGD data was obtained with a Netsch 429 thermoanalyzer. In all cases, standard platinum or aluminium (DSC) crucibles were used. The DSC crucibles were equipped with a lid having a pin-hole in the centre. Alumina was employed as reference material in DTA and DSC experiments.

Owing to the high molecular weight of vapor-phase zinc acetate the quadrupole MS system[14] connected to our TGA-7 apparatus could not be used. The evolved gas analysis (EGA) of zinc acetate had to be performed with a separate Kratos MS 80 RF high-resolution mass spectrometer which has a heated inlet for solid samples. The temperature of the sample chamber was in the range 250–400 °C.

Results and discussion

Crystal structure of $Zn_4O(CH_3COO)_6$. The final atomic coordinates are listed in Table 2, while Table 3 gives the bond lengths and angles within

Table 2. Fractional coordinates and equivalent isotropic thermal parameters (×10^2) for $Zn_4O(CH_3COO)_6$.

Atom	x	y	z	U_{eq}[a]/Å^2
Zn	−0.06815(4)	−0.06815(4)	−0.06815(4)	3.98
O(1)	0	0	0	3.31
O(2)	−0.0476(2)	−0.0476(2)	−0.1832(2)	5.67
C(1)	0.2192(5)	0	0	4.59
C(2)	0.3105(5)	0	0	5.57

[a] $U_{eq} = 1/3 \sum_i \sum_j U_{ij} a_i^* a_j^* \mathbf{a}_i \mathbf{a}_j$

Table 3. Bond lengths (Å) and bond angles (°) within the $Zn_4O(CH_3COO)_6$ molecule.

O(1)–Zn	1.936(1)
O(2)–Zn	1.946(4)
Zn–Zn^{i}	3.162(1)
O(2)–C(1)	1.252(5)
C(1)–C(2)	1.497(11)
O(2)–O(2)^{ii}	2.207(6)
O(2)–O(2)^{iii}	3.145(6)
O(1)–Zn–O(2)	111.1(1)
O(2)–Zn–O(2)^{iii}	107.8(1)
Zn–O(2)–C(1)	132.4(6)
O(2)–C(1)–C(2)	118.2(4)

Symmetry code: none: *x, y, z*; (*i*): *x, ȳ, z̄; x̄, y, z̄; x̄, ȳ, z*; (*ii*): *x̄, ȳ, z*; (*iii*): *z, x, y*.

the complex. Our X-ray work confirms the earlier structural reports concerning the unit cell dimensions, space group and the tetrahedral arrangement of Zn atoms,[4–9] as well as the isostructurality with the Be compound.[15] The tetrahedral arrangement of zinc atoms around the central oxygen is highly symmetrical (Fig. 1 and Table 3). Each zinc atom is also tetrahedrally coordinated by four oxygen atoms: three from different bidentate acetato groups, with the fourth one being

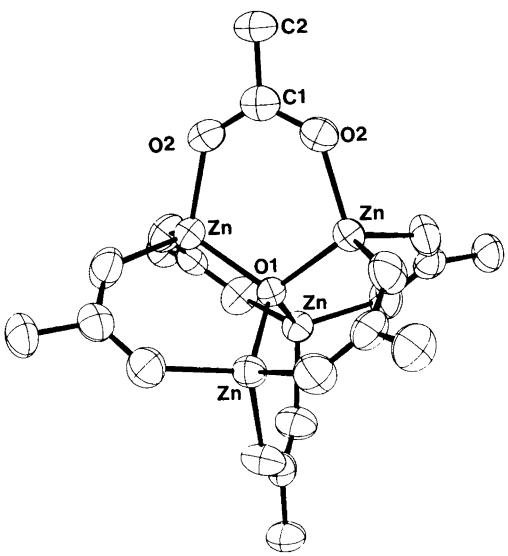

Fig. 1. A perspective view of the $Zn_4O(CH_3COO)_6$ complex.

the central oxygen. The Zn–O distance involving the central oxygen is slightly shorter [1.936(1) Å] than the other Zn–O distances, which are 1.946(4) Å. A reversed trend in distances was observed in the beryllium compound [1.664(4) and 1.624(10) Å].[15] The Zn–O distances of 1.936 and 1.946 Å may be compared with those observed in ZnO [1.973(2) and 1.992(7) Å], where the zinc atoms are also tetrahedrally coordinated.[16]

The distances within the acetato groups are normal and comparable to those found in the beryllium complex. For instance, the C–C and C–O bond lengths in the Zn complex are 1.497(11) and 1.252(5) Å, respectively, while the corresponding values in the Be compound are 1.500(6) and 1.264(8) Å (Table 3 and Ref. 15). In contrast to the distances associated with the strong intramolecular bonds, the intermolecular distances are long, viz. >4.3 Å between the non-hydrogen atoms. This indicates only very weak interactions and partly explains the unusual thermal properties.

The structural chemistry of oxygen-centered metal complexes (metallo complexes) has been discussed by Bergerhoff and Paeslack,[17] and more recently by Kauffman *et al.*[18] $M_4O(LL)_6$ type complexes, with $Zn_4O(CH_3COO)_6$ and $Be_4O(CH_3COO)_6$ as representative examples, may be classified as two-shell compounds because, in addition to the M_4O entity, there are chelating ligands coordinating to the metal. Table 4 lists the $M_4O(LL)_6$ complexes as well as other M_4O compounds for which X-ray structural data are available. In all cases M is a relatively small divalent cation. The majority of the compounds contain Cu^{2+} as the metal coordinating to the central oxygen, other divalent ions being Be^{2+}, Zn^{2+} and Mg^{2+}. The Cu_4O arrangement is apparently a stable configuration, as indicated by the existence of the oxide Cu_4O.[37] Trivalent ions, however, appear to prefer planar trigonal coordination, as in e.g. $[Fe_3O(CH_3COO)_6(H_2O)_3]\cdot ClO_4$,[19] $[Fe_3O(CH_3COO)_6(4\text{-Mepy})_3]\cdot C_6H_6$,[20] and $[Cr_3O(CH_3COO)_6(H_2O)]ClO_4\cdot 6H_2O$.[21]

Thermal behaviour. When zinc acetate dihydrate is slowly heated in air or nitrogen it first dehydrates, after which more or less complete volatilization follows. The sequence and extent of thermally induced reactions are strongly influenced by experimental conditions such as sample

Table 4. Compounds containing the M_4O tetrahedron.

(a) $M_4O(LL)_6$ type compounds

Compound	M_4O tetrahedron			MO_4 tetrahedron	Ref.
	M–O/Å	M–M/Å	M–O–M/°	M–O/Å	
$Zn_4O(CH_3COO)_6$	1.936(1)	3.162(1)	109.5	1.946(4)	Present work
$Zn_4O(BO_2)_6$	2.01	3.28	109.5	1.84	27
$Be_4O(CH_3COO)_6$	1.666(4)	2.721	109.5	1.624(10)	15

(b) Other compounds

Compound	M_4O tetrahedron			Ref.
	M–O/Å	M–M/Å	M–O–M/°	
$Cu_2O(SeO_3)$ (cubic)	1.916(4)–1.970(4)			28
$Cu_2O(SeO_3)$ (monoclinic)	1.933(3)–1.974(3)			28
$Cu_4O(SeO_3)_3$ (monoclinic)	1.889(5)–1.968(6)			28
$Cu_4O(SeO_3)_3$ (triclinic)	1.907(4)–1.984(4)			28
$[(CH_3)_4N]_4[Cu_4OCl_{10}]$	1.95(1)	3.18(1)	109.0–109.7	29
	1.92(1)	3.14(1)		
$[teedH_2]_2[Cu_4OCl_{10}]$	1.911(6)	3.117	108.9(4)	30
	1.922(6)	3.119	108.8(1)	
Cu_4OCl_6 (3-quin)$_4$	1.915(5)–1.925(3)	3.120(2)–3.155(1)	108.9(2)–110.3(2)	31
Cu_4OCl_6 (2-Mepy)$_4$	1.86(2)–1.93(2)	3.041(6)–3.206(6)	106.3(8)–115.8(8)	32
$Cu_4OCl_6(TPPO)_4$	1.905(3)	3.110(3)	109.5	33
$Cu_4OCl_6(OPEt_3)_4$	1.896(10)	3.130(2)	110.3(3)	34
	1.919(4)	3.116(2)	108.6(3)	
Cu_4OCl_6 (py)$_4$	1.88(2)	3.09–3.11	108(1)–111(1)	35
	1.92(2)			
$Mg_4OBr_6 \cdot 4C_4H_{10}O$	1.952(8)	3.118	109.5	36

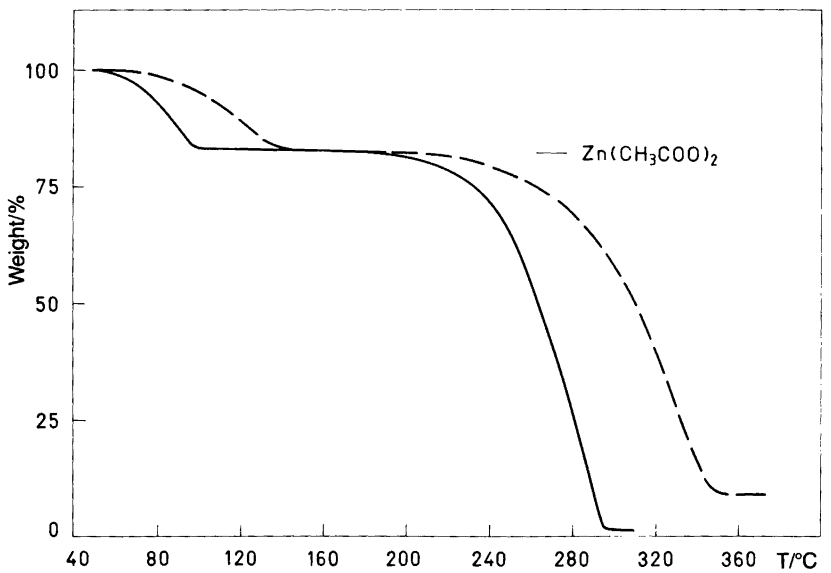

Fig. 2. Thermogravimetric (TG) curves for $Zn(CH_3COO)_2 \cdot 2H_2O$ recorded in dynamic nitrogen atmosphere using two heating rates: —— 5° min^{-1}, – – – 40° min^{-1}. Sample weight approx. 8 mg.

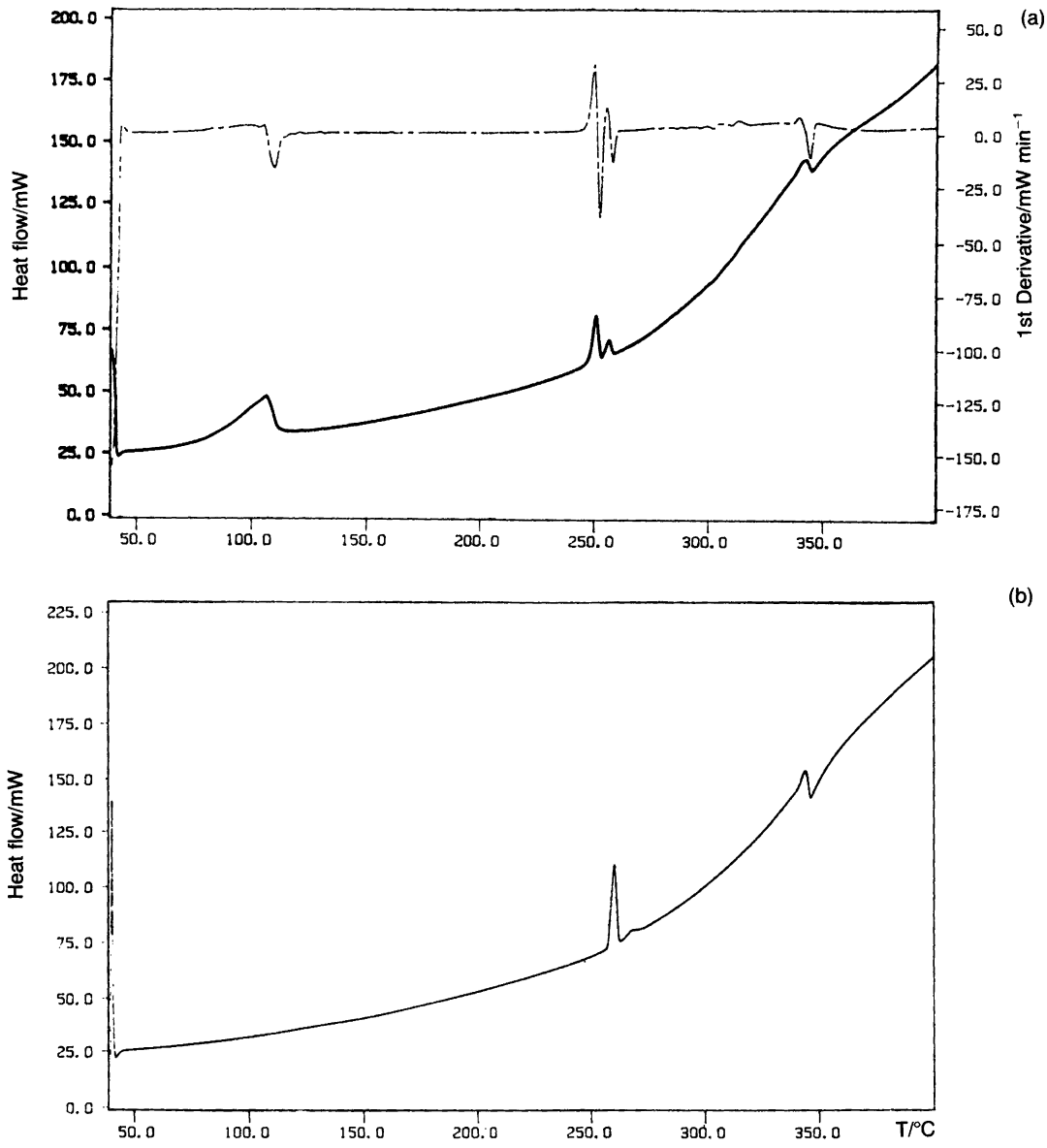

Fig. 3. Differential scanning calorimetric (DSC) curves in nitrogen for (a) $Zn(CH_3COO)_2 \cdot 2H_2O$ and (b) $Zn_4O(CH_3COO)_6$. Heating rate is 5° min^{-1}; sample weights 9.43 mg and 12.89 mg for (a) and (b), respectively. The first derivative is also depicted in (a) (broken line).

size, heating rate and crucible shape. The last-mentioned factor influences the self-generated atmosphere and may have a significant effect on the decomposition of $Zn(CH_3COO)_2 \cdot 2H_2O$.[22]

Fig. 2 depicts the TG curves in nitrogen for zinc acetate dihydrate at two heating rates, 5 and 40 °C min^{-1}, indicating that only with slow heating rates is there no or very little unvolatilized residue. When the heating rate is further increased to 200 °C min^{-1} the amount of residue

increases, being under these conditions 15 % of the original weight. Even at this heating rate a significant part is therefore volatilized as complete conversion of zinc acetate dihydrate to ZnO would lead to a residue of 37 weight %. The TG curve for $Zn_4O(CH_3COO)_6$ at low heating rate is very simple, showing only volatilization above 200 °C.

DSC curves recorded at 5 °C min^{-1} (Fig. 3a) clearly show that three endothermic processes take place when $Zn(CH_3COO)_2 \cdot 2H_2O$ is heated up to 300 °C. The first peak at 80–115 °C is due to dehydration and the second one, with maximum at 251 °C, is caused by melting of the anhydrous salt. The third peak centered at 257 °C is associated with the formation and melting of $Zn_4O(CH_3COO)_6$. When the DSC curve for $Zn_4O(CH_3COO)_6$ was recorded for comparison (Fig. 3b), the first and second maxima were absent and only the enhanced, third peak at 259 °C was visible. Above 260 °C the volatilization of $Zn_4O(CH_3COO)_6$ takes place, and the curb at 340 °C marks its termination. The main features of the simultaneously measured DTA/TG/EGD curves depicted in Fig. 4 are in complete agreement with the separate TG and DSC data, but in this case the sensitivity in enthalpy measurements is considerably lower.

Thermal decomposition of zinc acetate and the formation of oxoacetate have been studied in detail by McAdie, who used a thermoanalyzer for simultaneous TG and DTA measurements as well as a separate instrument for DTA curves.[23] He concluded that in dynamic nitrogen atmosphere anhydrous zinc acetate may decompose via two alternative routes [(1) or (2)]:

$$Zn(CH_3COO)_{2(s)} \rightarrow Zn(CH_3COO)_{2(l)} \rightarrow ZnO_{(s)} + CH_3COCH_{3(g)} + CO_{2(g)} \quad (1)$$

$$4Zn(CH_3COO)_{2(s)} \rightarrow Zn_4O(CH_3COO)_{6(s)} + (CH_3CO)_2O_{(g)} \rightarrow Zn_4O(CH_3COO)_{6(l)} \rightarrow 4ZnO_{(s)} + 3CH_3COCH_{3(g)} + 3CO_{2(g)} \quad (2)$$

Our conclusions differ from those of McAdie mainly in the interpretation of the effects associated with the doublet endothermic peak around 250 °C. We have found that when a sufficiently low heating rate is applied, zinc acetate forms oxoacetate which can be almost quantitively sublimed. The sequence of thermal reactions in nitrogen can then be summarized as follows:

$$4Zn(CH_3COO)_{2(s)} \rightarrow 4Zn(CH_3COO)_{2(l)} \rightarrow Zn_4O(CH_3COO)_{6(s)} + (CH_3CO)_2O_{(g)} \rightarrow Zn_4O(CH_3COO)_{6(l)} \rightarrow Zn_4O(CH_3COO)_{6(g)} \quad (3)$$

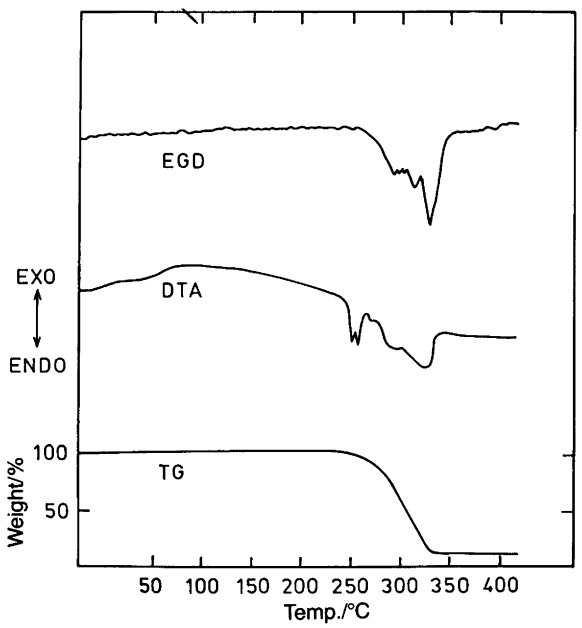

Fig. 4. Simultaneously recorded TG and DTA curves for $Zn(CH_3COO)_2$ in dynamic nitrogen atmosphere at a heating rate of 5 ° min^{-1}. In addition, the graph shows the evolved gas detection (EGD) curve. Sample weight 10.2 mg.

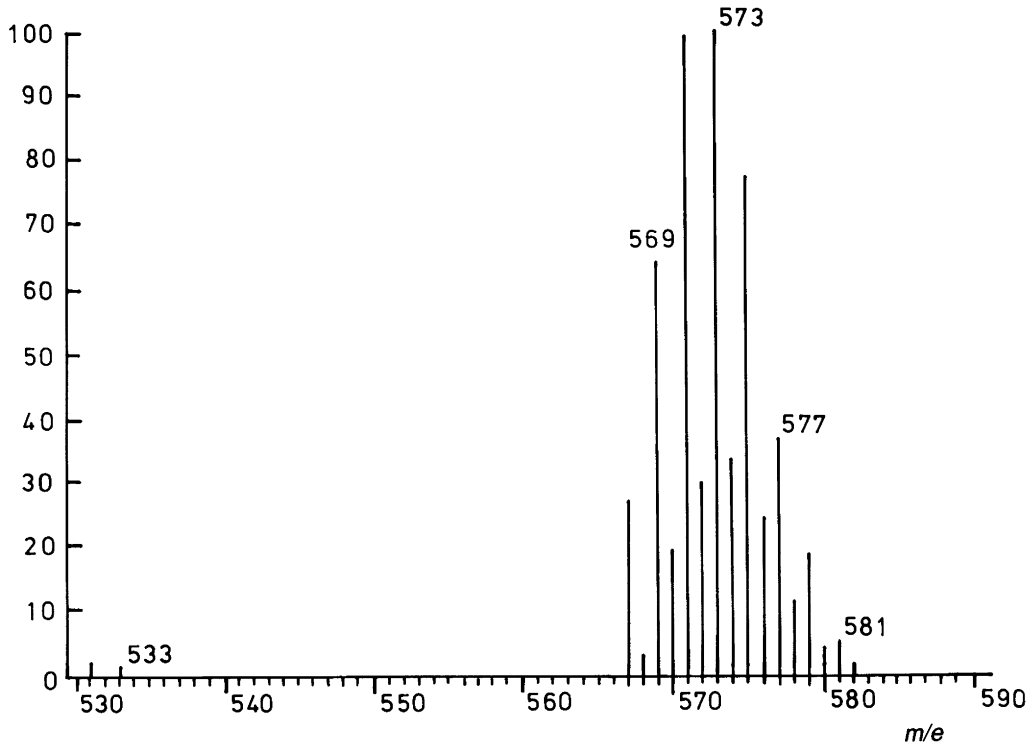

Fig. 5. The high resolution mass spectrum of $Zn(CH_3COO)_2 \cdot 2H_2O$ [or that of $Zn_4O(CH_3COO)_6$, which is identical]. The mass numbers around 205, 389 and 573 correspond to the dissociation fragments of $Zn_4O(CH_3COO)_6$, viz. $Zn_2O(CH_3COO)^+$, $Zn_3(CH_3COO)_3^+$ and $Zn_4O(CH_3COO)_5^+$.

Under these conditions only a small fraction of zinc acetate and/or oxoacetate decomposes to zinc oxide, thus making it possible to use zinc acetate as source material for vapor-phase growth of thin films in the ALE process. High growth rates, which are obtained for ZnS,[12] are probably due to the fact that a tetrameric zinc complex with a suitable geometry is involved in transport of the zinc atoms onto the substrate.

The mass spectrum of $Zn_4O(CH_3COO)_6$ has been studied by several authors, who have also published the fragmentation patterns for this compound[24–26] as well as for other related complexes.[24,25] Our MS results (Fig. 5) confirm the formation of higher molecular weight clusters from zinc acetate. The fragmentation pattern depends on experimental conditions.

Acknowledgements. The authors wish to thank Dr. H. Ruotsalainen for recording the high-resolution mass spectra, and Mr. P. Koskinen M.Sc. for recording the simultaneous TG/DTA curves. This work was supported through a grant from the Technology Development Centre (TEKES).

References

1. Urbain, G. and Lacombe, H. *Compt. Rend. 133* (1901) 874.
2. Ishibashi, M. and Motojima, M. *J. Chem. Soc. Jpn. 72* (1951) 100.
3. Barrat, R. S., Belcher, R., Stephen, W. I. and Uden, P. C. *Anal. Chim. Acta 57* (1971) 447.
4. Bragg, W. H. *Nature (London) 111* (1923) 532.
5. Bragg, W. H. and Morgan, G. T. *Proc. Roy. Soc. (London) A 104* (1923) 437.
6. Auger, V. and Robin, I. *Compt. Rend. 178* (1924) 1546.
7. Wyart, J. *Bull. Soc. Fr. Min. 49* (1926) 148.
8. Watanabe, T. and Saito, Y. *Nature (London) 163* (1949) 225.
9. Koyama, H. and Saito, Y. *Bull. Chem. Soc. Jpn. 27* (1954) 112.
10. Suntola, T., Antson, J., Pakkala, A. and Lindfors, S. *SID 80 Digest* (1980) 109.

11. Antson, H., Grasserbauer, M., Hamilo, M., Hiltunen, L., Leskelä, M. and Niinistö, L. *Fresenius' Z. Anal. Chem. 322* (1985) 175.
12. Tammenmaa, M., Koskinen, T., Hiltunen, L., Leskelä, M. and Niinistö, L. *Thin Solid Films 124* (1985) 125.
13. Pakkanen, T. A., Nevalainen, V., Lindblad, M. and Makkonen, P. *Surf. Sci. 188* (1987) 456.
14. Hiltunen, L., Härkönen, K., Leskelä, M., Niinistö, L. and Soininen, P. *To be published.*
15. Tulinsky, A., Worthington, L. R. and Pignataro, E. *Acta Crystallogr. 12* (1959) 623.
16. Abrahams, S. C. and Bernstein, J. L. *Acta Crystallogr., Sect. B 25* (1969) 1233.
17. Bergerhoff, G. and Paeslack, J. *Z. Kristallogr. 126* (1968) 112.
18. Kauffman, G., Karbassi, M. and Bergerhoff, G. *J. Chem. Educ. 61* (1984) 729.
19. Anzerhofer, K. and Deboer, J. J. *Rec. Trav. Chim. Pays-Bas 88* (1969) 286.
20. Woehler, S. E., Wittebort, R. J., Oh, S. M., Hendrickson, D. N., Inniss, D. and Strouse, C. E. *J. Am. Chem. Soc. 108* (1986) 2938.
21. Chang, S. C. and Jeffrey, G. A. *Acta Crystallogr., Sect. B 26* (1970) 673.
22. Hug, P., Oswald, H. R. and Tammenmaa, M. *Unpublished results.*
23. McAdie, H. G. *J. Inorg. Nucl. Chem. 28* (1966) 2801.
24. Mead, W. L., Reid, W. K. and Silver, H. B. *J. Chem. Soc., Chem. Commun.* (1968) 573.
25. Charalambous, J., Copperthwaite, R. G., Jeffs, S. W. and Shaw, D. E. *Inorg. Chim. Acta 14* (1975) 53.
26. Sipachev, V. A., Reshetova, L. N., Nekrasov, Yu. S. and Sil'vestrova, S. Yu. *Org. Mass. Spectrom. 15* (1980) 192.
27. Smith, P., Garcia-Blanco, S. and Rivoir, L. *Z. Kristallogr. 115* (1961) 460.
28. Effenberger, H. and Pertlik, F. *Monatsh. Chem. 117* (1986) 887.
29. Bertrand, J. A. and Kelley, J. A. *Inorg. Chem. 8* (1969) 1982.
30. Belford, R., Fenton, D. E. and Truter, M. R. *J. Chem. Soc., Dalton Trans.* (1972) 2345.
31. Dickinson, R. C., Helm, F. T., Baker, W. A., Jr., Black, T. D. and Watson, W. H., Jr. *Inorg. Chem. 16* (1977) 1530.
32. Gill, N. S. and Sterns, M. *Inorg. Chem. 9* (1970) 1619.
33. Bertrand, J. A. *Inorg. Chem. 6* (1967) 495.
34. Churchill, M. R., DeBoer, B. G. and Mendak, S. J. *Inorg. Chem 14* (1975) 2496.
35. Kilbourn, B. T. and Dunitz, J. D. *Inorg. Chim. Acta 1* (1967) 209.
36. Stucky, G. and Rundle, R. E. *J. Am. Chem. Soc. 86* (1964) 4821.
37. Guan, R., Hashimoto, H., Kuo, K. H. and Yoshida, T. *Acta Crystallogr., Sect. B 43* (1987) 343.

Received August 19, 1987.